

Growth of germanium on Au(111): formation of germanene or intermixing of Au and Ge atoms?

Received 00th January 20xx,
Accepted 00th January 20xx

Esteban D. Cantero^a, Lara M. Solis^b, Yongfeng Tong^c, Javier D. Fuhr^a, María Luz Martiarena^a, Oscar Grizzi^a and Esteban A. Sánchez^a

DOI: 10.1039/x0xx00000x

www.rsc.org/

Supplementary Information

Au atoms at the top Ge layer analysed with Ne projectiles

The use of Ar⁺ projectiles at relatively low energies (such as 4 keV) in recoiling observation is appropriate to enhance the sensitivity to changes in the crystallography of the top layer due to the large shadowing and focussing effects. This shadowing effect completely precludes observation of Au recoils along the compact direction $[\bar{1}01]$ of the clean surface. On the other hand, the Au recoil peak along $[\bar{2}11]$ appears enhanced due to focussing. This focussing effect makes more complex any quantitative determination of coverage. The use of lighter projectiles at higher energies results in smaller shadow cone radius and therefore the trajectories are less affected by focussing. Fig. SI-1 shows spectra along the two main directions for Ne at 12 keV scattering off both the clean surface and the high coverage Ge layer, for which a LEED pattern similar to that reported in ref. ¹ (Fig. 3(c) of main text) was observed. In correspondence with the measurements using Ar projectiles, with Ne we also observe the decrease of the Au peak along the $[\bar{2}11]$ direction and the increase of this peak along the $[\bar{1}01]$ direction after evaporation. Note that the new Au peaks have a contribution right at the position of the single collision (true Au direct recoil) indicated by a dashed line, which further demonstrates that in the Au sample covered with a multilayer of Ge, there are Au atoms at the top of this layer that are more accessible to the incident beam than in the clean (pure) Au surface, i.e., less shadowed and thus allowing true direct collisions. An accurate determination of surface composition is difficult; however an estimation can

be obtained from the ratio of the Ge/Au peak areas weighted by the corresponding cross section. Since the focussing effects cannot be avoided completely, in order to increase the statistical significance of our result we acquired spectra for different incidence and azimuthal angles and averaged the value of the ratio in the angular region where the focusing and shadowing were less important. The resulting value of the Ge/Au coverage ratio, after including the corresponding cross sections was of about 2 Ge atoms for every Au atom.

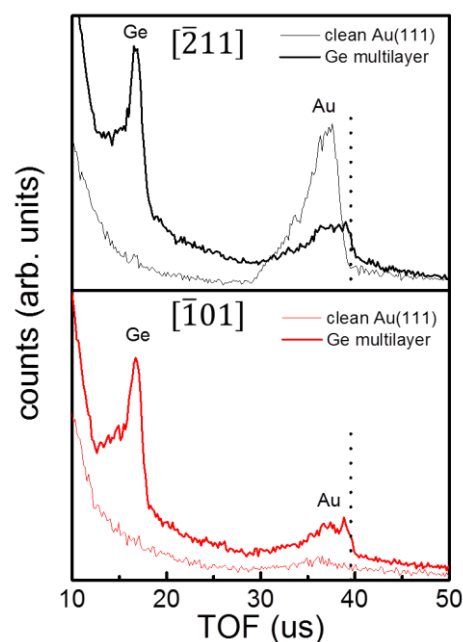


Fig. SI-1 TOF-DRS spectra recorded by 12 keV Ne⁺ ions along the $[\bar{2}11]$ and $[\bar{1}01]$ directions at 20° incidence. The spectra with thin lines correspond to the clean surface, whereas the thicker ones to the high coverage Ge layer.

For the clean surface, the shadowing effect is so important that when the measurement is taken at grazing angles (about 5°) no Au recoil peak is observed, even along the $[\bar{2}11]$ direction. However, for the Ge covered surface clear peaks due to both Ge and Au are observed at 5° (Fig. SI-2), which are

^a Centro Atómico Bariloche, Comisión Nacional de Energía Atómica CNEA, Consejo Nacional de Investigaciones Científicas y Técnicas CONICET. Instituto Balseiro, Universidad Nacional de Cuyo.

^b Instituto Balseiro, Universidad Nacional de Cuyo.

^c Université de Paris Sud, Institut des Sciences Moléculaires d'Orsay, UMR 8214 CNRS Université Paris Sud, Université Paris Saclay, Bâtiment 351, Orsay 91405, France. Synchrotron SOLEIL - L'Orme des Merisiers, Saint-Aubin - BP 48, 91192 GIF-sur-YVETTE CEDEX, France.

consistent with the strong corrugation of the surface seen in the STM image.

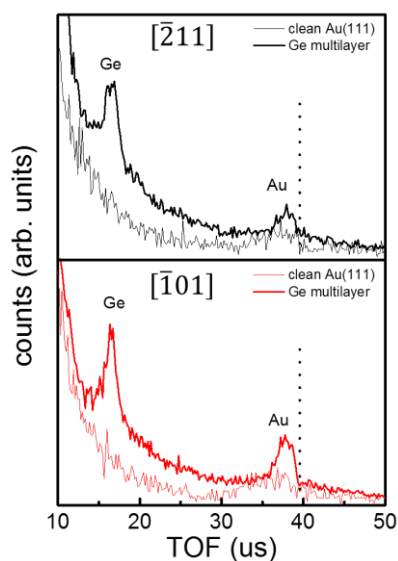


Fig. SI-2 TOF-DRS spectra recorded by 12 keV Ne^+ ions along the $[\bar{2}11]$ and $[\bar{1}01]$ directions at 5° incidence. The spectra with thin lines correspond to the clean surface, whereas the thicker ones to the high coverage Ge layer.

LEED patterns of the monolayer Ge film for different energies

We present on Figs. SI-3 (a) to (d) the LEED patterns of the monolayer Ge film just after 30 min evaporation and before annealing the sample, for different electron energies. The LEED patterns obtained after annealing at 520 K are shown in Figs. SI-4 (a) to (d).

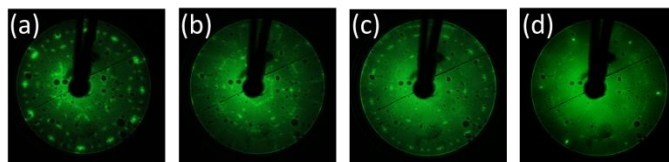


Fig. SI-3 LEED patterns for 30 min evaporation time with sample at 470 K prior to post-annealing. Electron energies were (a) 20.5 eV, (b) 35.5 eV, (c) 44.5 eV and (d) 74.5 eV.

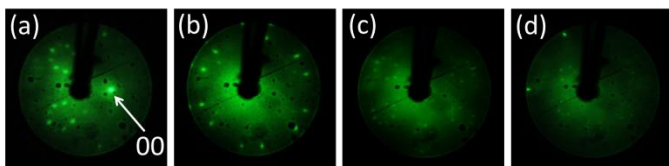


Fig. SI-4 LEED patterns for 30 min evaporation time with sample at 470 K after annealing at 520 K. Electron energies were (a) 19.5 eV, (b) 20.3 eV, (c) 35.0 eV and (d) 57.4 eV. Pattern of panel (a) is slightly rotated to show (00) spot.

Coexistence of Au and Ge atoms in the same atomic layer

Here we discuss in more detail the conclusion derived from Fig. 4 of the main text concerning the coexistence of Au and Ge atoms in the same layer for all coverages, including the

submonolayer regime: a) The small incident current density used in typical spectra (as indicated in the experimental section) produces negligible sputtering, i.e., extended measurements (taking 10 or more consecutive spectra) produces no change of the herringbone LEED pattern and the resulting TOF-DRS spectra is the same. b) For Ar projectiles at 4.2 keV the shadowing effects are so strong that they prevent observation of Au atoms along the $[\bar{1}01]$ direction for the clean Au surface, as seen in Fig. 1 of the main text. One can take many consecutive spectra, without annealing in between, and the spectra along this direction will not show the appearance of an Au recoil peak. This property of negligible damage allows the study of more sensitive surfaces like those covered by organic molecules, as it has been described in many reports, see for example, ref. ². c) The adsorption of sulphur on the Au(111) surface reported by our group in ref. ³ is an example of how TOF-DRS can detect the migration (or not) of Au atoms into the adsorbed layer. In Fig. 4 of this reference, one can clearly see that for low S coverage, below ~ 0.3 ML, the S peak presents characteristics of an absorption over the substrate atoms, while the Au atoms present the same crystallographic dependence of the clean surface, that is no Au atoms are detected along the $[\bar{1}01]$ while they are clearly detected along the open direction $[\bar{2}11]$. At higher S coverages, an alloyed surface is formed and both S and Au from the top layer become detectable along both directions, showing the high sensitivity of the technique to the migration of Au atoms into the adsorbed layer.

6x6 moiré type pattern

During the acquisition of STM images for the multilayer Ge film we observed, on one occasion, a structure which resembled a moiré pattern (Figs. SI-5 (a) and (b)), having an hexagonal symmetry, with an $n \times n$ structure with n of the order of 5. The distance between spots is of about 0.35 nm, which is neither a multiple integer of the distances on the germanene unit cell nor of the ones on the substrate unit cell. The average distance between the brighter zones of the moiré pattern is 1.73 nm, equivalent to a row of six Au atoms on the $[\bar{1}01]$ direction of the Au(111) substrate. The maximum height corrugation was of 0.03 nm. The 2D-FFT of Fig SI-5(b) is presented in Fig. SI-5(c), where the $n \times n$ structure can be clearly observed on the symmetry and arrangement of the spots of the transformed image.

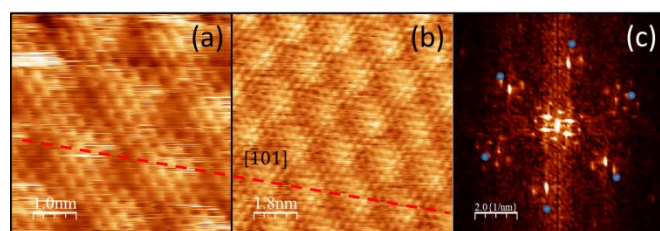


Fig. SI-5 6x6 moiré-type pattern observed after the depositing the Ge multilayer. (a) and (b) show STM images, with the dashed red line indicating the $[\bar{1}01]$ direction. (c) 2D-FFT of image (b).

DFT calculations details

The DFT calculations have been carried out within the slab-supercell approach by using the Vienna ab initio simulation program (VASP).^{4,5} The one-electron Kohn–Sham orbitals are expanded in a plane-wave basis set, and electron-ion interactions are described through the PAW_PBE pseudopotentials.⁶ The sampling of the Brillouin zone is carried out according to the Monkhorst–Pack method.⁷ The chosen cutoff energy is 400 eV. Electron smearing is introduced following the Methfessel–Paxton technique⁸ with $\sigma = 0.1$ eV, and all the energies are extrapolated to 0 K. The convergence of the energy is kept always on the order of 10^{-4} eV, and the minimization of the forces is assured up to the order of 10^{-1} eV/nm. For the exchange–correlation term, we used the PBEsol approximation⁹ which gives a lattice parameter for bulk Au of 4.078 Å which is in excellent agreement with the experimental value of 4.08 Å at room temperature.

The adsorption energy per Ge atom was calculated as:

$$E_{\text{ads}} = - \left[\frac{E_{\text{Ge/Au(111)}} - E_{\text{Au(111)}} - N_{\text{Au}} E_{\text{bulk Au}}}{N_{\text{Ge}}} - E_{\text{Ge}} \right] \quad (\text{S1})$$

where $E_{\text{Ge/Au(111)}}$ is the total energy of the relaxed configuration, $E_{\text{Au(111)}}$ is the total energy of the clean surface, N_{Au} is the number of adatoms (for $N_{\text{Au}} > 0$) or Au vacancies (for $N_{\text{Au}} < 0$) in the unit cell of the last layer, N_{Ge} is the number Ge atoms in the unit cell of the last layer, $E_{\text{bulk Au}}$ is the energy per atom of bulk Au, and E_{Ge} is the energy of an isolated Ge atom. The results for the considered configurations are shown in table S1. Note that of the studied cases the lowest-energy configuration corresponds to a $\sqrt{19} \times \sqrt{19}$ unit cell which is very close to the configuration proposed for Si/Pt(111) in¹⁰, with 6 Ge atoms and 15 Au atoms in the topmost layer of the unit cell. Moreover, this more compact alloy layer has a larger distance ($\sim 8\%$) to the Au(111) substrate and has a large corrugation (~ 0.13 Å). At present we were unable to correlate clearly these calculated configurations (individually or mixed) with the results of the complex LEED patterns measured for the initial stages of the adsorption. This is an interesting point that needs to be clarified before attempting a more realistic calculation of the germanene multilayer, but goes beyond the scope of the present work.

Table S1: Adsorption energy per Ge atom as calculated with Eq. (S1).

Unit cell	description	N_{Ge}	N_{Au}	$E_{\text{ads/Ge atom}}$ (eV)
3x3	adsorbed Ge	1	0	4.83
3x3	substitutional Ge	1	-1	4.86
3x3	3 substitutional Ge	3	-3	4.97
$(\sqrt{7} \times \sqrt{7})R19.1^\circ$	structure 3 of ref. ¹¹	6	0	4.96
$(\sqrt{7} \times \sqrt{7})R19.1^\circ$	structure 6 of ref. ¹¹	4	2	5.05

$(\sqrt{7} \times \sqrt{7})R19.1^\circ$	3 substitutional Ge	3	-3	5.13
$(\sqrt{7} \times \sqrt{7})R19.1^\circ$	3 substitutional Ge + 1 interstitial Au	3	-2	5.15
$(\sqrt{19} \times \sqrt{19})R23.4^\circ$	7 substitutional Ge + 2 interstitial Au	7	-5	5.20
5x8		15	-10	5.24
$(2\sqrt{19} \times 2\sqrt{19})R53.4^\circ$		28	-20	5.26
$(\sqrt{19} \times \sqrt{19})R23.4^\circ$	6 substitutional Ge + 2 interstitial Au	6	-4	5.28

References

- 1 María E. Dávila and Guy Le Lay, *Scientific Reports* 2016, **6**, 20714.
- 2 J. W. Rabalais, "Principles and Applications of Ion Scattering Spectrometry". Wiley–Interscience Series on Mass Spectroscopy. **2003**. ISBN 0-471-20277-0.
- 3 E. Tosi, G.D. Ruano, S. Bengió, L. Salazar Alarcón, E.A. Sánchez, M. Khalid, O. Grizzi, M.L. Martiarena, and G.E. Zampieri, *Nucl. Instr. and Meth. B* 2013, **315**, 55.
- 4 G. Kresse and J. Hafner, *Phys. Rev. B* 1993, **47**, 558.
- 5 G. Kresse and J. Hafner, *Phys. Rev. B* 1994, **49**, 14251.
- 6 J. P. Perdew, K. Burke, and M. Ernzerhof, *Phys. Rev. Lett.* 1996, **77**, 3865.
- 7 H. Monkhorst and D. Pack, *Phys. Rev. B* 1976, **13**, 5186.
- 8 M. Methfessel and A. T. Paxton, *Phys. Rev. B* 1989, **40**, 3616.
- 9 J. P. Perdew, A. Ruzsinszky, G. I. Csonka, O. A. Vydrov, G. E. Scuseria, L. A. Constantin, X. Zhou, and K. Burke, *Phys. Rev. Lett.* 2008, **100**, 136406.
- 10 M. Švec, P. Hapala, M. Ondráček, P. Merino, M. Blanco-Rey, P. Mutombo, M. Vondráček, Y. Polyak, V. Cháb, J. A. Martín Gago and P. Jelinek. *Phys. Rev. B* 2014, **89**, 201412(R).
- 11 M.E. Dávila, L. Xian, S. Cahangirov, A. Rubio and G. Le Lay, *New J. Phys.* 2014, **16**, 095002.